The Property and Photocatalytic Performance Comparison of Graphene, Carbon Nanotube, and C60 Modified TiO2 Nanocomposite Photocatalysts

Shaozheng Hu,[*] Fayun Li, and Zhiping Fan

Institute of Eco-environmental Sciences, Liaoning Shihua University, Fushun 113001, P.R. China
[*]E-mail: hushaozheng001@163.com

A series of carbon nanotube, C60, and graphene modified TiO2 nanocomposites were prepared by hydrothermal method. X-ray diffraction, N2 adsorption, UV-Vis spectroscopy, photoluminescence, and Electrochemical impedance spectra were used to characterize the prepared composite materials The results reveal that incorporating TiO2 with carbon materials can extend the adsorption edge of all the TiO2-carbon nanocomposites to the visible light region. The photocatalytic activities were tested in the degradation of 2,4,6-trichlorophenol (TCP) under visible light. No obvious difference in essence was observed in structural and optical properties among three series of carbon modified TiO2 nanocomposites. Three series of carbon materials modified TiO2 composites follow the analogous tentative reaction mechanism for TCP degradation. GR modified TiO2 nanocomposite exhibits the strongest interaction and the most effective interfacial charge transfer among three carbon materials, thus shows the highest electron-hole separation rate, leading to the highest photocatalytic activity and stability.

Key Words : Carbon nanotube, C60, Graphene, TiO2, Visible light

Introduction

TiO2, as a charming heterogeneous photocatalyst, has been widely investigated because of its optical-electronic properties, low-cost, chemical stability, and non-toxicity. However, there are two aspects limiting its application. TiO2 can be activated only by ultraviolet (UV) irradiation, the energy of which makes up only 3-5% of the solar light. On the other hand, over 90% photoexcited electrons and holes recombine, making most of the excitation useless.[1] Therefore, it is highly desirable to develop TiO2-based photocatalysts with high electron/hole separation rate and visible light activity.

The composite of TiO2 and carbon materials, particularly carbon nanotube (CNT), has attracted much attention in recent years.[2] Hoffmann *et al.*[3] proposed that the photo-generated electrons in the space-charge regions may be transferred into CNT, and the holes remain on TiO2, thus retarding the recombination of electrons and holes. Besides, CNT can provide high surface area and peculiar functional groups for the efficient adsorption of reactants and may act as photosensitizer. The formation of Ti-O-C bonds between TiO2 and CNT can shift the absorption edge into visible light region which obviously promote the photocatalytic performance under visible light. Furthermore, CNT could function for controlling the morphology of TiO2 nanoparticles.[4] It is known that C60 possesses high electron affinity and its electronic structure is similar to carbon nanotube.[5] One of the most attractive properties of C60 in electron-transfer processes is that it can arouse a rapid photoinduced charge separation effectively and restrain charge recombination.[6]

Thus, the combination of TiO2 and C60 can provide an ideal system to achieve the enhanced charge separation by photo-induced electron transfer.

Graphene (GR), as a new allotrope of carbon, has attracted an enormous amount of interest from both theoretical and experimental scientists since its discovery in 2004 by Geim and co-workers.[7] GR is a two-dimensional sp2-hybridized carbon nanosheet, which possesses many unique properties such as a very high theoretical specific surface area (~2600 $m^2 \cdot g^{-1}$), high mobility of charge carriers, and good mechanical strength.[8-10] Very recently, GR-based nanocomposites have been widely explored in many fields, including biosensors, nanoelectronics, intercalation materials, drug delivery, catalysis, supercapacitors, and polymer composites.[9-14] With regard to the region of photocatalysis, GR also catches the eyes of researchers in this field and promotes great interest to synthesize GR-semiconductor nanocomposites as photocatalysts for target applications.[15,16] It is shown that CNT, C60, and GR have many similar structure and electronic properties in common. Therefore, it is reasonable to raise a fundamental question: are they similar in promoting the photocatalytic performance of semiconductors when we use them to assemble carbon-semiconductor composite photocatalysts? In this work, the CNT, C60, and GR modified TiO2 nanocomposites were prepared by a hydrothermal method. The properties and photocatalytic performances of prepared nanocomposites were compared each other. It is hoped that this work could promote more objective understanding on the analogy and difference of these three carbon allotropes, CNT, C60, and GR on the rational synthesis and photoactivity improvement of semiconductor-carbon composites.

Experimental

Preparation and Characterization. Carbon nanotubes and C_{60} were purchased from Shenzhen Nanotech Port Co., Ltd., China and Yongxin Chemical Reagent Company. Graphene oxide (GO) was synthesized from natural graphite powder by a Hummers' method.[17] The preparation of carbon (GR, CNT, and C_{60}) modified TiO_2 nanocomposite photocatalysts is as follows. A certain amount of carbon materials (0.2, 0.5, 1.5, and 3 wt %) was sonicated in a mixed solution of 10 mL ethanol and 20 mL deionized water for a long time to ensure the thorough dispersion of carbon materials. Then, another solution (1.7 mL tetrabutyl titanate and 10 mL ethanol) was added dropwise to the above solution of carbon materials under stirring. After 3 h, the suspension was transferred into a 50 mL Teflon-lined autoclave and kept at 200 °C for 15 h. During the hydrothermal process, GO is reduced to GR.[18,19] The obtained precipitates were centrifuged and washed with deionized water until the pH value was neutral. After that, the solid samples were dried at 60 °C in oven and noted as GR-x, CNT-x, and C_{60}-x, where x stands for the weight ratio of carbon material to TiO_2. For comparison, neat TiO_2 was prepared following the same procedure without addition of carbon material.

XRD patterns of the prepared TiO_2 samples were recorded on a Rigaku D/max-2400 instrument using Cu-Kα radiation (λ = 1.54 Å). Nitrogen adsorption was measured at −196 °C on a Micromeritics 2010 analyzer. All the samples were degassed at 393 K before the measurement. BET surface area was calculated according to the adsorption isotherm. UV-Vis spectroscopy measurement was carried out on a Jasco V-550 spectrophotometer, using $BaSO_4$ as the reference sample. PL spectra were measured at room temperature with a fluorospectrophotometer (FP-6300) using an Xe lamp as excitation source. Electrochemical impedance spectra (EIS) made from these as-made materials were measured via an EIS spectrometer (EC-Lab SP-150, BioLogic Science Instruments) in a three-electrode cell by applying 10 mV alternative signal versus the reference electrode (SCE) over the frequency range of 1 MHz to 100 mHz. The cyclic voltammograms were measured in 0.1 M KCl solution containing 2.5 mM $K_3[Fe(CN)_6]/K_4[Fe(CN)_6]$ (1:1) as a redox probe with the scanning rate of 20 mV/s in the same three electrode cell as EIS measurement.

Photocatalytic Reaction. Photocatalytic TCP degradation was performed as follows. In a typical procedure, 0.1 g TiO_2 powders were dispersed in 100 mL solution of TCP (initial concentration $C_0 = 60 \times 10^{-6}$ g·mL^{-1}) in an ultrasound generator for 10 min. The suspension was transferred into a self-designed glass reactor, and stirred for 30 min in darkness to achieve the adsorption equilibrium. The concentration of TCP at this point was considered as the absorption equilibrium concentration $C_{0'}$. The adsorption capacity of a catalyst to TCP was defined by the adsorption amount of TCP on the photocatalyst (C_0-$C_{0'}$). In the photoreaction under visible light irradiation, the suspension was exposed to a 400 W high-pressure sodium lamp with UV cutoff filter (λ

> 420 nm), and air was bubbled at 130 mL/min through the solution. All runs were conducted at ambient pressure and 30 °C. The conversion of TCP was determined using an Agilent 1100 series HPLC operated in isocratic mode under the following conditions: methanol-water (80% : 20%); flow rate 1 mL·min^{-1}; temperature 25 °C; Column Phenomenex Luna 10 μ Phenyl-Hexyl, 4.6 mm × 250 mm; detector UV at 254 nm; injection volume 5 μL.

Results and Discussion

Figure 1 shows the photocatalytic activities of prepared TiO_2 nanocomposites under visible light. It is noted that dark condition without illumination or illumination in the absence of catalyst did not lead to the TCP decomposition, indicating the presence of both illumination and catalyst was necessary for efficient photocatalytic degradation. Unsurprisingly, neat TiO_2 exhibited very low photocatalytic activity because of the low visible light absorption (not shown). For carbon materials modified TiO_2 catalysts, TCP degradation rate improved obviously. CNT-0.5, C_{60}-0.5, and GR-1.5 exhibited the highest degradation rates for three series of carbon materials modified TiO_2 catalysts (72%, 76%, and 90%). It is indicated that CNT and C_{60} modified TiO_2 catalysts exhibited comparable activity, which is lower than that of GR modified TiO_2. In order to clear what cause the activity difference among three series of carbon materials modified TiO_2 catalysts, CNT-0.5, C_{60}-0.5, and GR-1.5 were selected for the further analysis.

The XRD patterns of the as-prepared neat and carbon materials modified TiO_2 catalysts are shown in Figure 2. It is shown that all of the TiO_2-carbon nanocomposites exhibit similar XRD patterns. The diffraction peaks of all samples match well with the anatase TiO_2 (JCPDS No. 21-1272). Compared with the standard card of anatase TiO_2, it is obvious that three different kind of carbon materials modification have no obvious influence on the TiO_2 characteristic peaks, which can be ascribed to two reasons. On the one hand, the addition amounts of carbon materials in the nanocomposites are very low. On the other hand, the main
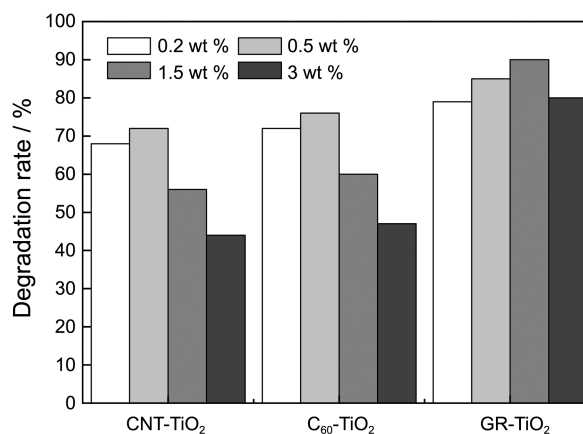

Figure 1. Photocatalytic performances of prepared samples in the degradation of TCP under visible light irradiation.
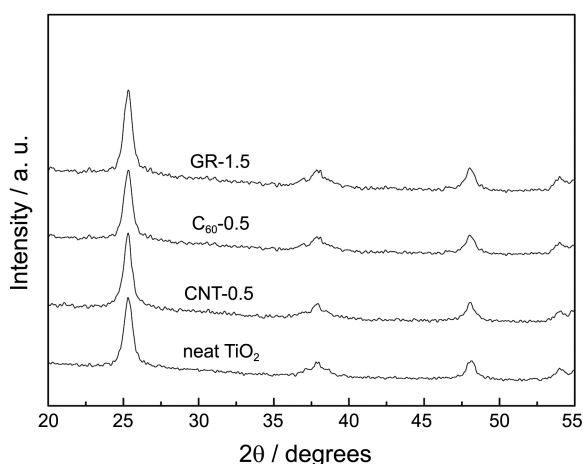
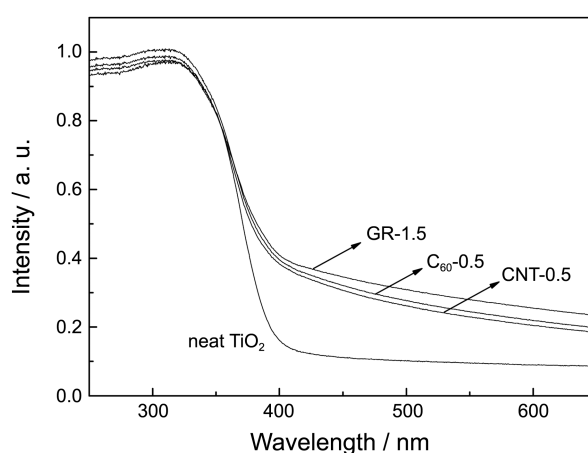**Figure 2.** XRD patterns of the as-prepared neat and carbon materials modified TiO₂ catalysts.

Figure 3. UV-Vis diffuse reflectance spectra of as-prepared neat and carbon materials modified TiO₂ catalysts.

characteristic peaks of GR and CTN are located at 25.0° and 26.2° which probably shadowed by the (101) peak anatase TiO₂ (25.3°), which is consistent with the previous reports.[20] The particle sizes of the as-prepared nanocomposites were calculated by their XRD patterns according to the Debye-Scherrer equation and shown in Table 1.[21] Obviously, carbon materials modified TiO₂ catalysts exhibit the similar particle size with neat TiO₂. Generally, the ability of adsorption, desorption, and diffusion of reactants and products are mainly determined by the S_{BET} and pore volume of catalyst.[22] Therefore, a catalyst with high specific surface area (S_{BET}) and big pore volume is significant to the enhancement of catalytic performance.[23] The S_{BET} and pore volume of neat TiO₂ are 168 m^2g^{-1} and 0.37 cm^3g^{-1}, which are very close to that of carbon materials modified TiO₂ catalysts (Table 1). This is reasonable because, with such a small carbon amount, the surface area and porosity are mainly dominated by TiO₂ ingredients. Based on above results, it is concluded that three series of carbon modification did not change the crystal phase, particle size, and structural property of TiO₂ catalyst.

To study the optical properties of as-prepared neat and carbon materials modified TiO₂ catalysts, UV-Vis spectra were measured, as shown in Figure 3. It is shown obviously that the addition of CNT, C₆₀, and GR all induce the significant increased light absorption intensity in the whole visible light region. Such phenomenon were reported by previous literatures.[24,25] The absorption curves of three series of carbon materials modified TiO₂ are almost the same,

indicating that the optical properties have no essential difference among them. The absorption intensity starts to increase rapidly at 400 nm for neat TiO₂, corresponding to the intrinsic band gap absorption of anatase TiO₂. For carbon materials modified TiO₂ catalysts, the red shifts of the absorption edges are observed, which is consistent with previous reports.[26-28] This is proposed to correspond to the formation of Ti-O-C bond between TiO₂ and carbon materials similar to that observed for the carbon-doped TiO₂ composites.[29] The band-gap energies calculated according to the method of Oregan and Gratzel were 3.1, 2.9, 2.9, and 2.86 eV for neat TiO₂, CNT-0.5, C₆₀-0.5, and GR-1.5, indicates that carbon materials modified TiO₂ catalysts exhibited much narrowed band-gap energies.[30] Such slight narrowed band-gap energy of GR-1.5 compared with other carbon modified TiO₂ catalysts suggests that the interaction between TiO₂ and GR was the strongest among three series of carbon modified TiO₂ nanocomposites.[25] The absorption of carbon materials modified TiO₂ composites in the visible light region is of great importance for its practical application since it could be activated by visible light.

In order to compare the interaction between TiO₂ and three carbon materials, 0.1 g CNT-0.5, C₆₀-0.5, and GR-1.5 were dispersed in 10 mL water and sonicated for 10 min respectively, and then the suspensions were obtained. For GR-1.5, the as-prepared nanocomposite in suspension began to sink to the bottom after resting for a while. After 2 h, the solution became clear, indicating that the simultaneous subsiding of TiO₂ and GR. This suggests that the GR in the solution are completely coupled on the surface of TiO₂ nanoparticles to form a TiO₂-GR nanocomposite. However, for CNT-0.5 and C₆₀-0.5 suspensions, partial carbon materials rose up to the surface immediately. The formed TiO₂-carbon nanocomposites sink to the bottom within 1.5 h, leaving the partial colloidal TiO₂ suspension. This hints a stronger interaction between the TiO₂ and GR compared with other carbon materials.

During the recombination process of photo-induced charge carriers, a certain amount of chemical energy is released,
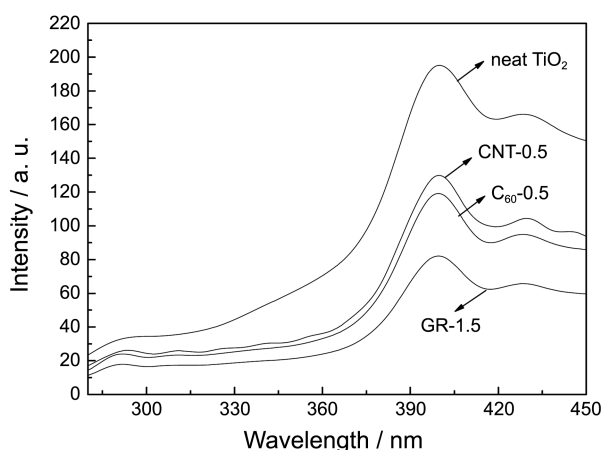
Table 1. Particle sizes, S_{BET}, Pore volume, and TCP adsorption amount of prepared TiO₂ catalysts

Sample	Size (nm)	S_{BET} (m^2g^{-1})	Pore volume (cm^3g^{-1})	Adsorption amount (ppm)
Neat TiO₂	12.2	168	0.37	5.2
CNT-0.5	12.5	172	0.35	5.5
C₆₀-0.5	11.8	169	0.36	5.4
GR-1.5	12.6	174	0.37	5.5

Figure 4. Photoluminescence emission spectra of as-prepared neat and carbon materials modified TiO₂ catalysts.

Figure 5. EIS spectra of CNT-0.5, C₆₀-0.5, and GR-1.5.

following by transform to heat or light energy. The light energy is dissipated as radiation, which results in a luminescence emission of semiconductor, called the PL phenomenon. PL is a highly sensitive technique used to provide information on charge separation/recombination of photo-induced charged carriers.[31] In general, the lower PL intensity, the higher separation rates of photogenerated e^-/h^+ pairs, thus the higher the photocatalytic activity. Figure 4 presents a comparison of PL spectra of as-prepared neat and carbon materials modified TiO₂ catalysts. It is shown that all the catalysts exhibit the similar PL curves. Carbon materials modified TiO₂ exhibit the lower PL intensities compared with neat TiO₂. This should be due to the interaction between TiO₂ and carbon materials which cause the charge transfer occurred between them, leading to the lower electron-hole recombination rate. It is known that most of the electrons and holes recombine within a few nanoseconds in the absence of scavengers. If scavengers, such as CNT, C₆₀, and GR, are present to trap the electrons or holes, the electron-hole recombination can be suppressed, leading to a photoluminescence quenching. Besides, GR-1.5 exhibits much lower PL intensity than that of CNT-0.5 and C₆₀-0.5. This is probably due to that stronger interaction between TiO₂ and GR than CNT and C₆₀ causes its charge transfer more effectively, which is consistent with UV-Vis result.

Electrochemical impedance spectroscopy (EIS) is a very useful tool to characterize the charge-carrier migration, thus was used to further confirm the interfacial charge transfer effect of as-prepared TiO₂ nanocomposites. Figure 5 shows the EIS Nyquist plots of the as-prepared carbon materials modified TiO₂ composites under visible light irradiation. GR-1.5 shows much decreased arc radius compared with CNT-0.5 and C₆₀-0.5. The reduced arc radius indicates diminished resistance of working electrodes, suggesting a decrease in the solid state interface layer resistance and the charge transfer resistance across the solid-liquid junction on the surface by forming hybrid structures of TiO₂ with graphene.[32] Since the radius of the arc on the EIS spectra reflects the migration rate occurring at the surface, it suggests that a more effective separation of photogenerated electron-hole
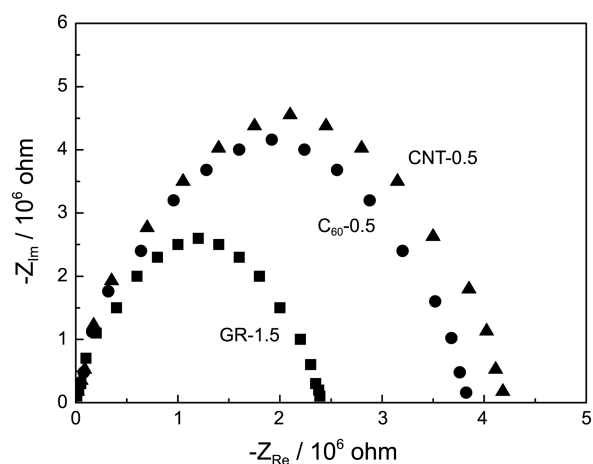
pairs and a faster interfacial charge transfer occurs on GR-1.5 surface under this condition.[33] Combine with the PL results, it is concluded that the GR modified TiO₂ nanocomposite exhibits the most effective interfacial charge transfer among three carbon materials, thus shows the highest electron-hole separation rate, leading to the highest photocatalytic degradation rate.

It is known that the adsorption capacity of catalyst is a key factor which influences its catalytic performance. The adsorption of TCP on neat TiO₂, CNT-0.5, C₆₀-0.5, and GR-1.5 were measured by the equilibrium adsorption capacity, and shown in Table 1. Obviously, the absorption amount of all the samples are very close, which should be due to their similar S_{BET} and pore volume values. In order to further understand the underlying reaction mechanism for the photocatalytic degradation of TCP over the as-prepared carbon modified TiO₂ photocatalysts, a series of controlled experiments with addition of different scavengers for the photogenerated radical species have been investigated (Figure 6). When the hydroxyl radicals (·OH) scavenger,[34,35] tert-butyl alcohol (TBA), is added to the reaction system of the three carbon materials modified TiO₂ nanocomposites, the TCP degradation only slight decreased compared with
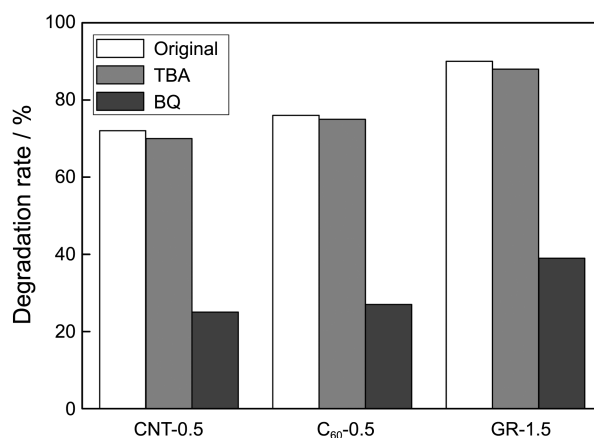

Figure 6. Controlled experiments using different radical scavengers for the photocatalytic degradation of TCP under visible light.

the original experiments without the radical scavengers. This indicates hydroxyl radical is not the main active oxygen species for this oxidation reaction. However, when the radical scavenger, benzoquinone (BQ), for superoxide radical species ($O_2^{\cdot-}$) is added into the reaction system,[36,37] the degradation rate decreased dramatically, indicating $O_2^{\cdot-}$ is mainly responsible for the TCP degradation. Therefore, it is deduced that the active oxygen species for TCP degradation over three series of carbon materials modified TiO₂ catalysts are the same.

For the practical application of photocatalysts, the mineralization ratio in the catalysis process is a key issue. The photocatalytic degradation of organic compound is a complex process, and many intermediate products are produced, especially when the initial substrate is complicated. Many intermediate products are more harmful to human health than the initial pollutant, so a thorough decomposition of the pollutant is necessary. The mineralization ability of prepared catalysts to TCP molecules was evaluated by monitoring the changes of TOC in the reaction systems. Figure 7 shows the evolution of TOC during the TCP degradation under visible light over prepared materials. The TOC removal rate follows the order: neat TiO₂ < CNT-0.5 < C₆₀-0.5 < GR-1.5, which is consistent with degradation rate. The ratio of degradation rate of TCP to TOC removal rate represents the mineralization ratio. The calculated results indicated that the mineralization ratios for CNT-0.5, C₆₀-0.5, and GR-1.5 were very close (0.74, 0.76, and 0.77). Summing up the above discussion, we propose that three series of carbon materials modified TiO₂ composites follow the analogous tentative reaction mechanism for TCP degradation.

In order to check the photocatalytic stability of prepared carbon-TiO₂ nanocomposites, the photocatalytic performances of fresh and reused catalysts were investigated (Figure 8). No obvious decrease in activity was observed for GR-1.5 after three cycles, indicating its good stability. However, for CNT-0.5 and C₆₀-0.5, the activities decreased obviously. This is probably due to that the interaction between TiO₂ and CNT or C₆₀ is not strong enough, leading to the structural
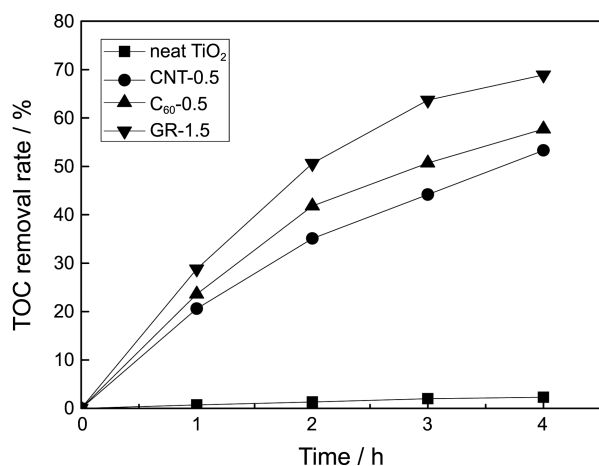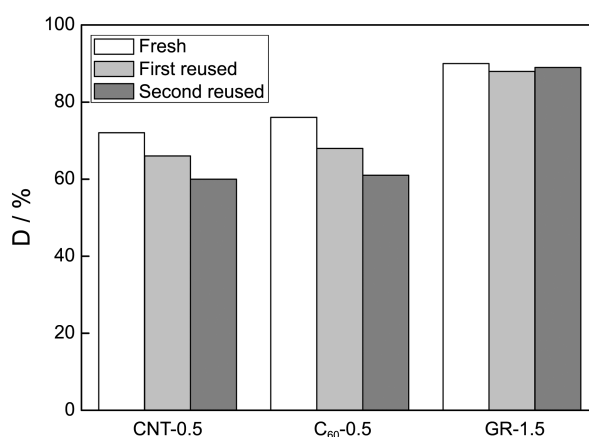

Figure 8. Photocatalytic stability of CNT-0.5, C₆₀-0.5, and GR-1.5.

damage during the reaction. In order to confirm our point of view, we observed the suspensions of fresh and reused CNT-0.5 and C₆₀-0.5 carefully. It was found that, compared with fresh CNT-0.5 and C₆₀-0.5, more carbon materials rose up to the surface for reused catalysts. This indicates that the structural damage of nanocomposite occurred, leading to more TiO₂ and carbon materials separated from each other. Therefore, it is confirmed that the structures of CNT-0.5 and C₆₀-0.5 are not as stable as that of GR-1.5.

Conclusion

A series of carbon nanotube, C₆₀, and graphene modified TiO₂ nanocomposites were prepared by hydrothermal method. The results reveal that incorporating TiO₂ with carbon materials can extend the adsorption edge of all the TiO₂-carbon nanocomposites to the visible light region. The optimal carbon amounts were 0.5, 0.5, and 1.5 wt % for carbon nanotube, C₆₀, and graphene modified TiO₂ nanocomposites. No obvious difference in essence was observed in structural and optical properties among three series of carbon modified TiO₂ nanocomposites. Three series of carbon materials modified TiO₂ composites follow the analogous tentative reaction mechanism for TCP degradation. GR modified TiO₂ nanocomposite exhibits the strongest interaction and the most effective interfacial charge transfer among three carbon materials, thus shows the highest electron-hole separation rate, leading to the highest photocatalytic activity and stability. It is hoped that this work could promote more objective understanding on the analogy and difference of these three carbon allotropes, CNT, C₆₀, and GR on the rational synthesis and photoactivity improvement of semiconductor-carbon composites.

Figure 7. Evolution of TOC during the course of TCP degradation under visible light over prepared materials.

References

1. Wang, X. D.; Caruso, R. A. *J. Mater. Chem.* **2011**, *21*, 20.
2. Woan, K.; Pyrgiotakis, G.; Sigmund, W. *Adv. Mater.* **2009**, *21*, 2233.
3. Hoffmann, M. R.; Martin, S. T.; Choi, W.; Bahnemann, D. W. *Chem. Rev.* **1995**, *95*, 69.
4. Xu, Y. J.; Zhuang, Y.; Fu, X. *J. Phys. Chem. C* **2010**, *114*, 2669.
5. Joumet, C.; Maser, W. K.; Bernier, P.; Loiseau, A.; de la Chapelle, M. L.; Lefrant, S.; Deniard, P.; Lee, R.; Fischer, J. E. *Nature* **1997**, *388*, 756.
6. Yu, G.; Gao, J.; Hummelen, J. C.; Wudl, F.; Heeger, A. J. *Science* **1995**, *270*, 1789.
7. Novoselov, K. S.; Geim, A. K.; Morozov, S. V.; Jiang, D.; Zhang, Y.; Dubonos, S. V.; Grigorieva, I. V.; Firsov, A. A. *Science* **2004**, *306*, 666.
8. Geim, A. K.; Novoselov, K. S. *Nature Mater.* **2007**, 6, 183.
9. Geim, A. K. *Science* **2009**, *324*, 1530.
10. Allen, M. J.; Tung, V. C.; Kaner, R. B. *Chem. Rev.* **2010**, *110*, 132.
11. Rao, C. N. R.; Sood, A. K.; Subrahmanyam, K. S.; Govindaraj, A. *Angew. Chem., Int. Ed.* **2009**, *48*, 7752.
12. Guo, S.; Dong, S. *Chem. Soc. Rev.* **2011**, *40*, 2644.
13. Xiang, Q.; Yu, J.; Jaroniec, M. *Chem. Soc. Rev.* **2012**, *41*, 782.
14. Liang, Y. T.; Hersam, M. C. *J. Am. Chem. Soc.* **2010**, *132*, 17661.
15. Zhao, D.; Sheng, G.; Chen, C.; Wang, X. *Appl. Catal., B* **2012**, *111-112*, 303.
16. Zhang, J.; Xiong, Z.; Zhao, X. S. *J. Mater. Chem.* **2011**, *21*, 3634.
17. Hummers, W. S.; Offeman, R. E. *J. Am. Chem. Soc.* **1958**, *80*, 1339.
18. Zhang, Y.; Tang, Z. R.; Fu, X.; Xu, Y. J. *ACS Nano* **2011**, *5*, 7426.
19. Pan, X.; Zhao, Y.; Liu, S.; Korzeniewski, C. L.; Wang, S.; Fan, Z. Y. *ACS Appl. Mater. Interfaces* **2012**, *4*, 3944.
20. Zhang, Y.; Tang, Z. R.; Fu, X.; Xu, Y. J. *ACS Nano* **2010**, *4*, 7303.
21. Lin, J.; Lin, Y.; Liu, P.; Meziani, M. J.; Allard, L. F.; Sun, Y. P. *J. Am. Chem. Soc.* **2002**, *124*, 11514.
22. Liu, S. W.; Yu, J. G.; Jaroniec, M. *J. Am. Chem. Soc.* **2010**, *132*, 11914.
23. Yu, J. G.; Wang, G. H.; Cheng, B.; Zhou, M. H. *Appl. Catal. B* **2007**, *69*, 171.
24. Zhang, L. W.; Wang, Y. J.; Xu, T. G.; Zhu, S. B.; Zhu, Y. F. *J. Mol. Catal. A: Chem.* **2010**, *331*, 7.
25. Fan, W. Q.; Lai, Q. H.; Zhang, Q. H.; Wang, Y. *J. Phys. Chem. C* **2011**, *115*, 10694.
26. Zhu, P. L.; Nair, A. S.; Yang, S. Y.; Peng, S. J.; Elumalai, N. K.; Ramakrishna, S. *J. Photochem. Photobiol. A* **2012**, *231*, 9.
27. Mu, S.; Long, Y. Z.; Kang, S. Z.; Mu, J. *Catal. Commun.* **2010**, *11*, 741.
28. Shah, Md. S. A. S.; Park, A. R.; Zhang, K.; Park, J. H.; Yoo, P. J. *ACS Appl. Mater. Interfaces* **2012**, *4*, 3893.
29. Sakthivel, S.; Kisch, H. *Angew. Chem. Int. Ed.* **2003**, *42*, 4908.
30. Oregan, B.; Gratzel, M. *Nature* **1991**, *353*, 737.
31. Nakajima, H.; Mori, T.; Shen, Q.; Toyoda, T. *Chem. Phys. Lett.* **2005**, *409*, 81.
32. He, B. L.; Dong, B.; Li, H. L. *Electrochem. Commun.* **2007**, *9*, 425.
33. Huang, Q. W.; Tian, S. Q.; Zeng, D. W.; Wang, X. X.; Song, W. L.; Li, Y. Y.; Xiao, W.; Xie, C. S. *ACS Catal.* **2013**, *3*, 1477.
34. Zhang, N.; Fu, X.; Xu, Y. J. *J. Mater. Chem.* **2011**, *21*, 8152.
35. Zhang, N.; Liu, S.; Fu, X.; Xu, Y. J. *J. Phys. Chem. C* **2011**, *115*, 22901.
36. Stylidi, M.; Kondarides, D. I.; Verykios, X. E. *Appl. Catal., B* **2004**, *47*, 189.
37. Raja, P.; Bozzi, A.; Mansilla, H.; Kiwi, J. *J. Photochem. Photobiol. A* **2005**, *169*, 271.